CHAPTER 66

PREDICTIVE EQUATIONS REGARDING COASTAL TRANSPORTS

by

D. H. SWART*

1. INTRODUCTION

Morphological changes are the result of gradients in longshore and onshore-offshore sediment transport. The coastal engineer is continually faced with engineering problems in which a quantitative knowledge of these morphological changes is required. For this purpose predictive equations have been developed for both longshore and onshore-offshore sediment transport, which are being used in practical applications. In this paper a few of these predictive techniques, as well as one of their typical applications, viz. to a beachfill problem, will be discussed.

2. ONSHORE-OFFSHORE SEDIMENT TRANSPORT

2.1 *General*

The basics of Swart's *onshore-offshore sediment-transport theory* were described in detail in [14]. A paper about this subject was presented at the 1974 Coastal Engineering Conference in Copenhagen [13]. Subsequently it had become clear that the computational method described in [14]is too complicated for normal use, and that it could be modified to simplify the computations, without affecting the results significantly. In the present paper a summary will be given of the basic principles underlying the theory, as well as of the modified computational approach used at present. In Chapter 4 the method will be applied to a *beachfill problem*, to illustrate one of its typical applications.

2.2 *Underlying principles*

(1) The development in a normal beach profile is characterized into *three definite* zones, (Figure 1), each with its own transport mechanism, viz.

(a) the *backshore*, i.e. the area above the wave run-up limit in which *"dry" transport* takes place,
(b) a *developing profile* (D-profile) where a combination of *bed load- and suspended load-transport* takes place, and
(c) a *transition area*, seawards of the D-profile, and landwards of the point where sediment motion by wave action is initiated, where normally only *bed load* transport takes place.

(2) The most basic assumption in the schematization of onshore-offshore sediment transport is that the developing profile (D-profile) will eventually reach a *stable situation* under persistent wave attack. This stable situation implies both an *equilibrium form* and an *equilibrium position* of the beach profile. This last concept is illustrated in Figure 2, where the *schematized* volume of sediment in the D-profile is plotted as a function of time. Similar variations are found for the different locations in the D-profile, thus also confirming the equilibrium form concept.

(3) The sediment transport rates into (or out of) the D-profile from (or to) the backshore and the transition area ($S_e(t)$ and $S_t(t)$ respectively) form the boundary conditions for the computation of profile changes in the D-profile. These transport rates were found in [14] to be given by :

*Coastal Engineering and Hydraulics Division
National Research Institute for Oceanology, South Africa

$$S_e(t) = s_e W_e \exp\left(\frac{-s_e t}{\delta_e}\right) \quad \ldots (2.1)$$

and

$$S_t(t) = s_t W_t \exp\left(\frac{-s_t t}{\delta_t}\right) \quad \ldots (2.2)$$

where s_e and s_t are the backshore- and transition area-coastal constants and

$$\begin{aligned} W_e &= L_e\ (t=o) - L_e\ (t=\infty) \\ W_t &= L_t\ (t=\infty) - L_t\ (T=o) \\ t &= \text{time} \end{aligned} \quad \ldots (2.3)$$

The other variables are defined in Figure 1.

(4) With the aid of the assumption in step (2) above, the rate of onshore-offshore sediment transport S_{yit} at a specific location i in the profile at any time t can be shown to be a function of the difference between the values of a profile characteristic P at time t (P(t)) and time $t = \infty$ (P(∞)).

$$S_{yit} \propto P(\infty) - P(t) \quad \ldots (2.4)$$

(see Figure 3)

Experiments showed that the best description of the transport is found if the profile characteristic is taken to be a horizontal length in the profile $(L_2 - L_1)_{it}$.

$$S_{yit} = s_{ym} \left(\frac{s_{yi}}{s_{ym}}\right) (W_i - (L_2 - L_1)_{it}) \quad \ldots (2.5)$$

where s_{ym} and s_{yi} are transport coefficients and

$$(L_2 - L_1)_{it} \xrightarrow[\infty]{t} W_i \quad \ldots (2.6)$$

The meaning of $(L_2 - L_1)_{it}$ and the geometry of the beach profile at time t is defined in Figure 1. Relationships are presented in [13], whereby s_{ym}, (s_{yi}/s_{ym}) and W_i, as well as the limits of the D-profile (i.e. the area in which equation (2.5) is valid) can be found in terms of the boundary conditions.

(5) A subsequent study of the given relationships indicated that the computation of time-dependent profile development can be significantly improved and simplified if it can be assumed that at each location i in the developing profile the same fraction f_{it} of the total transport $(\int_o^\infty S_{yit}\, dt)$ of sediment passing that location until time $t = \infty$, will have occurred at any given time t, i.e.

$$f_{it} = \left\{\frac{\int_o^t S_{yit}\, dt}{\int_o^\infty S_{yit}\, dt}\right\} = f_t = \text{constant for all locations i in the developing profile at time t.} \quad \ldots (2.7)$$

The results of morphological tests with durations in excess of 1 000 hours, given in Figures 4 and 5, show that the above-mentioned assumption (equation (2.7)) is a good engineering approximation.

(6) With the principle of continuity of mass, and by using steps (1) - (5) above, it is possible to derive analytical expressions for the time variation of the length $(L_2 - L_1)_{it}$ and the sediment transport, viz.:

$$(L_2 - L_1)_{it} = W_i - (K_{ei} + K_{ti}) \exp(-X_b t) \quad \ldots (2.8)$$

$$S_{yit} = s_{yi} (K_{ei} + K_{ti}) \exp(-X_b t) \quad \ldots (2.9)$$

$$V_{yit} = \int_o^t S_{yit}\, dt = s_{yi} (K_{ei} + K_{ti})\, X_b^{-1} (1 - \exp(-X_b t)) \quad \ldots (2.10)$$

Substitution of equation (2.10) above into equation (2.7) yields an expression for f_t :

$$f_t = 1 - \exp(-X_b t) \quad \ldots (2.11)$$

where

$$K_{ei} = \frac{W_e \delta_e}{\delta_{1i}(X_b^{-1} X_i - 1)} \quad \ldots (2.12)$$

$$K_{ti} = \frac{W_t \delta_t}{\delta_{2i}(X_b^{-1} X_i - 1)} \quad \ldots (2.13)$$

$$X_b = \frac{s_e}{\delta_e} = \frac{s_t}{\delta_t} \quad \ldots (2.14)$$

$$X_i = \frac{\delta s_{yi}}{\delta_{1i} \delta_{2i}} \quad \ldots (2.15)$$

(7) The theory is valid, not only for perpendicular waves, but also for oblique wave attack. In the latter case the transport coefficients s_{yi} and s_{ym} are increased, to allow for the effect of the increase in shear stress at the bed, due to the presence of nearshore currents, generated by the oblique waves. The data used to derive the relationship for the increase in s_{yi} and s_{ym}, as presented in [14] and [13], was derived from model tests in which a strong rip-current formation was found. A subsequent study into the effect of the rip-currents on the increase in offshore transport, showed that the increase in transport, which is due to the presence of longshore currents alone, can best be written in terms of the increase (due to longshore currents) of the sediment mobility F (refer to [17] and [1]).

$$\frac{(s_{yi})_{wc}}{(s_{yi})_w} = \frac{(F_i)_{wc}}{(F_i)_w} \quad \text{(see Figure 6)} \quad \ldots (2.16)$$

where F_i is the sediment mobility at location i and the subscripts *wc* and *w* refer to *combined wave and current action* and *wave action only* respectively.

In order to comply with step (5) above, the mean value of equation (2.16) *over the whole area of profile development* will be applied to all transport coefficients.

$$\frac{(s_{yi})_{wc}}{(s_{yi})_w} = \overline{\left\{\frac{(F_i)_{wc}}{(F_i)_w}\right\}} \quad \ldots (2.17)$$

Keeping in mind the normal uncertainty factor in the *evaluation* of sediment transport data, it can be stated that the validity of equations (2.16) and (2.17) is proved by the data in Figure 6.

2.3. *Representative wave height*

The theory described above was derived and verified for regular wave attack. In order to make it generally applicable to prototype conditions, the effect of irregular waves on the theory must be known. The irregular waves will affect not the underlying principles, but the empirical predictive equations which will be described in section 2.4 below.

Observations showed that the higher waves in the wave spectrum will define the profile limits described in section 2.2, step (1) above. The *lower limits* of the *D-profile* and *transition area* respectively are both found by using the *significant* wave height in the empirical formulae derived for regular wave attack, whereas the *upper limit* of the D-profile is found from the regular-wave formula by using a wave with a height twice that of the significant wave height

If it is assumed that the transport-formulae are still applicable in the transport zones defined by these representative wave heights, the *single representative wave height* which will yield the *same resultant transport* as the spectrum, can be computed (the wave heights are assumed to be Raleigh-distributed).

The formulae for irregular wave attack, derived in this manner, and those for regular wave attack, will be given in section 2.4.

2.4 *Predictive equations*

The various equations needed for the application of the theory in section 2.2, will be summarized below for the sake of convenience.

2.4.1 *Limits of profile development* (refer to Figure 1)

The *upper limit* of the *backshore* is chosen at the highest level from which sediment can be eroded indirectly by wave action.

h_e *is chosen*

upper limit D-profile :

$$h_o = 7650 D_{50} \left[1 - \exp\left(-0.000143 \frac{H_{mo}^{0.488}\, T^{0.93}}{D_{50}^{0.786}}\right)\right] \qquad \ldots (2.18)$$

where H_{mo} = maximum wave height in the spectrum = $2(H_o)_{sign.}$; T is the wave period and D_{50} is the median particle diameter. For regular wave attack, such as in small-scale hydraulic models, $H_{mo} = H_o$.

lower limit D-profile

$$h_m = 0.0063 \lambda_o \exp\left(4.347 \frac{(H_o)_{sign.}^{0.473}}{T^{0.894} D_{50}^{0.093}}\right) \qquad \ldots (2.19)$$

where λ_o is the deepwater wave length. For regular wave attack $(H_o)_{sign} = H_o$.

lower limit transition area

The maximum orbital velocity at the bed at the location where initiation of sediment movement takes place (u_{SEGAR}), is found from the following formula, which represents the weighted mean of a number of different *initiation of movement*-Formulae. [12], [16].

$$u_{SEGAR} = 4.58\, D_{50}^{0.38}\, T^{0.043} \qquad \ldots (2.20)$$

The depth at which this velocity occurs is h_t. The corresponding wave length is λ_t. The first order wave representation of the orbital velocity can now be used to obtain a value for h_t/λ_t, whereafter it follows that :

$$h_t = \lambda_o \left(\frac{h_t}{\lambda_t}\right) \tanh\left(2\pi \left(\frac{h_t}{\lambda_t}\right)\right) \qquad \ldots (2.21)$$

In the case of irregular wave attack the significant wave height should be used for the computation of (h_t/λ_t). Finally, with the aid of equations (2.18), (2.19) and (2.21), it follows that :

$$\delta_e = h_e - h_o \qquad \ldots (2.22)$$

$$\delta = h_o + h_m \qquad \ldots (2.23)$$

$$\delta_t = h_t - h_m \qquad \ldots (2.24)$$

(see Figure 1).

2.4.2 *Equilibrium profile characteristics* (refer to [14] and [13])

The computation of the equilibrium length W_i is subdivided into two parts, viz. :

(1) the computation of a reference value W_r (=W_i at the still-water level), and

(2) the computation at all other locations in the D-profile of the ratio W_i/W_r.

re (1)

$$m_r = \frac{1.51 \times 10^{3}\, D_{50}^{1.06}\, H_o^{0.39}}{\lambda_o^{0.71}} + 0.11 \times 10^{-3} \left(\frac{\lambda_o}{H_o}\right) \qquad \ldots (2.25)$$

$$W_r = \frac{\delta}{2m_r} \qquad \ldots (2.26)$$

In the case of irregular wave attack, equation (2.25) is rewritten as :

$$m_r = \frac{1.21 \times 10^3 \, D_{50}^{1.06} \, (H_o)_{sign}^{0.39}}{\lambda_o^{0.71}} + 0.22 \times 10^{-3} \, \frac{\lambda_o}{(H_o)_{sign}} \qquad \ldots (2.27)$$

re (2)

For any location i in the D-profile the ratio W_i/W_r is given by :

$$W_i/W_r = 0.7\Delta_r + 1 + 3.97 \times 10^7 b \, D_{50}^2 \, \Delta_r^{1.36 \times 10^4 D_{50}} \qquad \ldots (2.28)$$

where $$\Delta_r = \frac{\delta_{1i} - h_o}{\delta} = \frac{h_m - \delta_{2i}}{\delta} \qquad \ldots (2.29)$$

and $$b = \begin{cases} 0 \; ; \; \Delta_r < 0 \\ 1 \; ; \; \Delta_r > 0 \end{cases} \qquad \ldots (2.30)$$

With the aid of equations (2.25) - (2.30) above the *form of the equilibrium D-profile*, measured relative to the position in the profile where $\delta_{1i} = 0$ (see Figure 1), can be written as :

$$Y_{i\infty} = W_r \, [2.1 \, z^2 - (1.4 + 2Q) \, z + P \, (1 - 2z)(h_r - z)^E \; EP \, (z^2 - z) \, (h_r - z)^{E-1} + (2Q - 0.7)] \qquad \ldots (2.31)$$

where $h_r = h_m/\delta$ ... (2.32)

$z = \delta_{2i}/\delta$ ... (2.33)

$Q = 0.7 \, h_r + 1$ ... (2.34)

$P = 3.97 \times 10^7 \, b \, D_{50}^2$ ... (2.35)

$E = 1.36 \times 10^4 \, D_{50}$ ... (2.36)

The *equilibrium slope* $\alpha_{t\infty}$ of the deposited material in the *transition area* can be found from the equation of Eagleson et al [6] :

$$\alpha_{t\infty} = \frac{\Delta Z_t}{\Delta L_t} \qquad \ldots (2.37)$$

$$\Delta L_t = 42.73 \, \frac{J}{K} \, \lambda_o \left[\ln (0.01335 - 0.0161 \, \frac{d}{\lambda_o}) + 0.7271 \, (\frac{d}{\lambda_o})^2 + 1.206 \, (\frac{d}{\lambda_o}) - 1.50 \right]_{(h_m + \Delta Z_t)/\lambda_o}^{h_m/\lambda_o} \qquad \ldots (2.38)$$

where ΔZ_t is a depth increment and ΔL_t is the horizontal distance in the equilibrium depositional profile between the depths bracketing ΔZ_t.

The values of the *schematized recession of the backshore* (W_e) and the *schematized growth of the transition area* (W_t) can be found by drawing up equations for :

(1) the conservation of mass (re Figure 7a)

(2) the geometrical form of the equilibrium profile (re (Figure 7b), and

(3) the distribution of the sediment in the transition area at equilibrium (re Figure 7b). The

reason why three equations are necessary to solve for the two unknowns W_e and W_t, is that δ_{tr} (see Figure 7a) is also an unknown.

2.4.3 *Coastal constants* (see [17])

At the elevation where $\delta_{1i} = 0.56$, the value of s_{yi} approximates s_{ym} very closely. s_{ym} is given by :

$$s_{ym} = \frac{D_{50}}{T} \exp\left[10.7 - 28.9\left\{(H_o)_{50}^{0.78}\,\lambda_o^{0.9}\,D_{50}^{-1.29}\left(\frac{(H_o)_{sign}}{h_m}\right)^{2.66}\right\}^{-0.079}\right] \quad \ldots (2.39)$$

where $(H_o)_{50}$ is the median deepwater wave height and $(H_o)_{sign}$ is the significant deepwater wave height. In the case of regular wave attack, both $(H_o)_{50}$ and $(H_o)_{sign}$ are replaced by H_o.
With the aid of section 2.2, step (5), it follows that :

$$X_b = \left(\frac{s_e}{\delta_e}\right) = \left(\frac{s_t}{\delta_t}\right) = \left\{\frac{(y_2 - y_1)_{io}}{W_{bi} + (y_2 - y_1)_{io}}\right\} X_i \quad \ldots (2.40)$$

with as a result

$$\frac{s_{yi}}{s_{ym}} = \frac{4\delta_{1i}\,\delta_{2i}}{\delta^2}\left[\frac{(y_2 - y_1)_{mo}}{W_{bm} + (y_2 - y_1)_{mo}}\right]\left[\frac{W_{bi} + (y_2 - y_1)_{io}}{(y_2 - y_1)_{io}}\right] \quad \ldots (2.41)$$

where $$W_{bi} = \left(\frac{\delta_e}{\delta_{1i}}\right) W_e + \left(\frac{\delta_t}{\delta_{2i}}\right) W_t \quad \ldots (2.42)$$

$$(y_2 - y_1)_{io} = W_i - (L_2 - L_1)_{io} \quad \ldots (2.43)$$

Subscript m refers to middepth ($\delta_{1i} = 0.56$) and subscript o refers to time t = 0.
The characteristic quantities K_{ei} and K_{ti} can now be found from equations (2.12) and (2.13) respectively.

2.4.4 *Mobility number*

(for a more detailed description of the mobility number and the following equations, reference should be made to [15] and [17]).

$$(F_i)_{wc} = \left\{\frac{v\, I_{wc}^n}{C_D^{\frac{1}{2}-n}\, C_h^n\, (\Delta_s\, D_{35})^{\frac{1}{2}}}\right\}_i \quad \ldots (2.44)$$

$$(F_i)_w = \left\{\frac{2^{-n}\, f_w^{n/2}\, u_o}{C_D^{\frac{1}{2}-n}\, C_h^n\, (\Delta_s\, D_{35})^{\frac{1}{2}}}\right\}_i \quad \ldots (2.45)$$

where $$I_{wc} = \left\{1 + \tfrac{1}{2}\left(\frac{\xi_J\, u_o}{v}\right)^2\right\}_i^{\frac{1}{2}} \quad \ldots (2.46)$$

$$\xi_{Ji} = \left\{C_h\left(\frac{f_w}{2g}\right)^{\frac{1}{2}}\right\}_i \quad \ldots (2.47)$$

$$C_{hi} = \left\{18 \log\left(\frac{12\, d}{r}\right)\right\}_i \quad \ldots (2.48)$$

$$C_{Di} = \left\{18 \log\left(\frac{10\, d}{D_{35}}\right)\right\}_i \quad \ldots (2.49)$$

$$f_{wi} = \left\{\exp\left(-5.977 + 5.213\left(\frac{a_o}{r}\right)^{-0.194}\right)\right\}_i \quad \ldots (2.50)$$

(if $f_{wi} > 0.3$; $f_{wi} = 0.3$)

r = hydraulic bed roughness

$$= 25\,\Delta_r\,(\frac{\Delta_r}{\lambda_r}) \qquad \ldots (2.51)$$

(See Figure 8)

a_o is the orbital excursion at the bed, Δ_r is the ripple height and λ_r is the ripple length.

$$n = 1 - 0.2432 \ln (D_{gr}) \qquad \text{(with } 0 \leqslant n \leqslant 1) \qquad \ldots (2.52)$$

$$D_{gr} = (\frac{g\,\Delta_s}{\nu^2})^{1/3} D_{35} \qquad \ldots (2.53)$$

D_{35} = particle diameter which is exceeded in size by 65% (in weight) of the total sample.

In the case of irregular wave attack the median wave height $(H_o)_{50}$ should be used in the equations (2.44) - (2.50).

2.5 *Computational Method*

The computation of *time-dependent profile changes* (Y_{it}) and *onshore-offshore sediment transport rates* S_{yit}, as well as of *integrated onshore-offshore transport rates* ($\int_o^t S_{yit}\,dt$) up to any time t, can all be performed by using the following simple procedure :

1) compute the *equilibrium condition*,
2) compute the value of the *fraction* f_t *as a function of time* with the aid of section 2.4,
3) combine 1) and 2) to *predict time-dependent conditions*.

In the case of *profile-prediction*, the *location* of the *equilibrium profile* can be predicted, because the *initial profile* is given and the *equilibrium profile form* as well as the values W_e *and* W_t can be computed from section 2.4. The position Y_{it} of the profile at elevation Z_i and time t is then given by:

$$Y_{it} = Y_{i\infty} + f_t\,(Y_{io} - Y_{i\infty}) \qquad \ldots (2.54)$$

(see Figure 9)

In the case of *transported-volume prediction* the total volume of transported material up to time $t = \infty$ ($V_{yi\infty}$) can be computed from equation (2.10) by putting $t = \infty$, whereafter V_{yit}, the total volume of sediment transported past the location in the profile with elevation Z_i, can be computed from :

$$V_{yit} = f_t\,V_{yi\infty} \qquad \ldots (2.55)$$

The *onshore-offshore sediment transport rate* at location i can also be found in terms of $V_{yi\infty}$ and f_t :

$$S_{yit} = V_{yi\infty}\,X_b\,(1 - f_t) \qquad \ldots (2.56)$$

3. LONGSHORE SEDIMENT TRANSPORT

3.1 *General*

Longshore sediment-transport computations can be used, either to gain an insight into the *overall sediment budget* of an area, or to study *detail problems* (such as deposition of sediment in an entrance channel to a harbour). The *total sediment load at various locations* will be needed in the first case, whereas the *vertical distribution of sediment load* (and specifically the division between bed and total load) will also be needed in the second case.

The available formulae for the prediction of longshore sediment transport rates can be classified into two groups, viz. :

(1) *overall predictors*, such as the *SPM-formula* and the *Galvin-formula*, and
(2) *detail predictors*, such as the *Bijker-formula* and the analogous *SWANBY-method*.
When a prediction of longshore sediment transport rates has to be made, it is useful to perform the computations with two or more of the available formulae, and to *base the final prediction on* the outcome of *all the results* obtained. In this chapter a detail-predictor method (SWANBY) will be described in detail, as well as a *modified version* of the SPM-predictor, which is used to back up the detail-predictor results.

3.2 *Overall predictors*

Although the overall predictors are by definition only applicable in areas with negligible longshore gradients, and cannot be used to obtain reliable estimates of the longshore transport rates in areas with strong longshore tidal flow, they can be useful in assessing the overall longshore sediment budget in an area. As such they can be used in conjunction with the detail predictors.
The SPM-formula, which relates the overall longshore transport rate S_{xtot} to a quantity resembling the longshore component of the wave-energy flux, is the best-known overall predictor available..This SPM-relationship can be rewritten to read :

$$S_{xtot} = K_o (T\,(H_o)^2_{rms}\,K_r^2 \sin\theta_b \cos\theta_b) \quad \text{(see [19])} \qquad \ldots (3.1)$$

where K_r is the refraction coefficient, θ_b is the angle between the wave crest and the shoreline at wave breaking, and K_o is a coefficient which is assumed to be constant.
However, as lighter material will be transported more readily than heavier materials under the same wave conditions, it is to be expected that K_o will be a function of the grain size of the bed material. A re-evaluation of the data given in [19] and [3] yielded Figure 10, from which a clear tendency can be seen for K_o to vary with grain size. Although a steeper curve is to be expected intuitively, the data suggests K_o to vary as :

$$K_o = 365 \times 10^4 \log\left(\frac{0.00146}{D_{50}}\right) \text{ for } 0.1\times10^{-3}\text{m} < D_{50} < 1.0\times10^{-3}\text{m} \qquad \ldots (3.2)$$

Equations (3.1) and (3.2) are normally used to back up computations performed with the detail predictor, which will be described in section 3.3.

3.3 *Detail predictors*

3.3.1 *Underlying principles*

In 1966 Bijker [2] published a method for the computation of the longshore sediment transport at any specific location in the coastal environment, which constituted a major breakthrough in Coastal Engineering. Bijker assumed that it will be possible to use, in the coastal environment, a sediment transport formula which had been developed for uniform flow conditions, provided that the shear stress terms in the chosen formula are adapted to incorporate the effect of the wave action. He chose as basis for this adaptation the formula of Frijlink, which was at the time a much-used formula in river-flow problems in the Netherlands. Although the resulting Bijker-Frijlink equation sometimes yielded unrealistic results, it has been used since then with a reasonable amount of success in numerous applications in the coastal environment. However, the insight into the fundamentals of sediment transportation under wave action has increased over the past decade. Furthermore, various evaluations of the available predictor methods revealed recently ([5], [7], [18], [20]) that there are more reliable methods for the computation of sediment transport under uniform flow conditions than the Frijlink-equation, which can also be used over a wider range of boundary conditions. Therefore, a new pre-

dictor method was developed by Swart [15] under the auspices of the Coastal Sediment Group of the Dutch Applied Coastal-Research Programme, for application in the coastal environment.
The basic differences between the new technique (called the SWANBY-method) and the old Bijker-Frijlink approach will be discussed below.

(1) The Frijlink-formula, used in the original approach, is a bed load formula. The total load was computed from the bed load by adding the suspended load, as computed with the aid of the Rouse/Einstein description of the vertical distribution of suspended sediment. The thickness of the bed layer is in such an approach an important parameter in the determination of the total load. Due to the uncertainty in the definition of the layer in which the bed load takes place, it will be more convenient to choose a total load formula as basis for computations in the coastal environment. If necessary, a definition can then be made of a bed layer thickness, and the amount of sediment transported in that layer can be computed.

(2) Various comparative investigations [5], [7], [18], [20], showed that the two most reliable total load formulae available for uniform flow conditions, are those of *Engelund-Hansen* and *Ackers-White*. Both these formulae give comparable results over a wide range of boundary conditions, the only exception being cases where the sediment transport rate was low (near initiation of motion). In such cases the *Engelund-Hansen method over-predicted* the transport rates, where Ackers-White showed a good comparison. *Engelund-Hansen will* thus *not yield proper scale relationships*, that can be used for the scaling of three-dimensional small-scale models. For the above-mentioned reasons the *Ackers-White approach was chosen* as the basic theory, which was to be adapted for use in the coastal environment.

(3) When evaluating the shear stress at the bed due to combined wave and current action, Bijker assumed the orbital velocity $u_{z'}$ at the edge of the viscous sublayer to be :

$$u_{z'} = p_B u_o \sin\left(\frac{2\pi t}{T}\right) \qquad \ldots (3.3)$$

where p_B = constant = 0.45 (see [2])

It is, however, to be expected that the effect of the wave motion on the shear stress will vary with a variation in the flow regime at the bed. Jonsson [9] defined the flow regime at the bed in terms of the ratio a_o/r where r is the hydraulic bed roughness and a_o the maximum wave particle excursion at the bed. Using Jonsson's work, it can be shown that

$$u_{z'} = p_J u_o \sin\left(\frac{2\pi t}{T}\right) \qquad \ldots (3.4)$$

where

$$p_J = \left(\frac{f_w}{2\kappa^2}\right)^{\frac{1}{2}} \qquad \ldots (3.5)$$

C_h is the Chezy-roughness value and f_w is the wave friction factor.
In the SWANBY-approach equation (3.4) was used instead of equation (3.3).

(4) In the Bijker-Frijlink approach the hydraulic bed roughness was taken equal to one-half the ripple height. A subsequent study [15] has shown the relative roughness (r/Δ_r) to vary with the ripple steepness Δ_r/λ_r (see Figure 8). This was used in the SWANBY-theory. It was shown in [15] that the thickness of the layer near the bed in which vortices (filled with sediment) are formed and diffused, is of the same order of magnitude as the hydraulic bed roughness r. The thickness of the layer in which bed load takes place was thereafter also assumed to be equal to the hydraulic bed roughness r.

(5) A comparative study of the various methods for the computation of the vertical distribution of suspended sediment $(\bar{c}_z/\bar{c}_r)$ in the coastal environment [15]showed that there is little difference

between the prediction of $\bar{c}_z/\bar{c}_r$ by various theories. The *best correlation* with data covering a wide range of boundary conditions in the coastal environment was, however, obtained with a theory in which the *diffusion coefficient* for solids ε was assumed to *vary linearly* over the depth. The corresponding variation in $\bar{c}_z/\bar{c}_r$ is :

$$\frac{\bar{c}_z}{\bar{c}_r} = \left(\frac{z}{r}\right)^{-b_1} \qquad \ldots (3.6)$$

where b_1 is a constant for each specific suspended sediment distribution over the depth.
With the assumption of a logarithmic variation in velocity over the depth, equation (3.6) yields an expression for the amount of suspended sediment which is transported, which is *easier to apply than any of the other* approaches tested. Due to these reasons it was decided to use equation (3.6) in the SWANBY-method instead of the Rouse/Einstein approach.

In Figure 11 longshore sediment transport rates, measured in a small-scale model, are compared with predicted transport rates, as given by the Bijker-Frijlink and SWANBY (Adapted Ackers-White) formulae. It is obvious that the SWANBY-method shows the better comparison with the data.

3.3.2 *Predictive equations*

The equations needed for the application of the SWANBY-method for the computation of the longshore sediment transport, will be given below.

total load

The total longshore sediment transport S_{xt} (bed plus suspended load) at any specific location is given by :

$$S_{xt} = \left(\frac{1}{1-p}\right) D_{35}\, v \left(\frac{C_h}{\sqrt{g}}\right)^{n} I_{wc}^{-n} \frac{C}{A^m} \{F_{wc} - A\}^m \qquad \ldots (3.7)$$

where $\left(\frac{1}{1-p}\right)$ = determined by the porosity of the bed, normally taken = 1.45 and v = uniform current velocity in the longshore direction. The values of C_h, I_{wc}, F_{wc} and n are defined in section 2.4.4 (equation (2.44), (2.46) - (2.53)). Furthermore

$$m = \frac{9.66}{D_{gr}} + 1.34 \qquad \ldots (3.8)$$

$$A = \frac{0.23}{D_{gr}} + 0.14 \qquad \ldots (3.9)$$

$$C = \exp\left[2.86 \ln (D_{gr}) - 0.4343 (\ln (D_{gr}))^2 - 8.128\right] \qquad \ldots (3.10)$$

The hydraulic bed roughness r is related to the ripple dimensions as given in equation (2.51). The ripple dimensions can either be known from observations or be computed from one of the available methods (for instance[11] and [15]).

bed load

The bed load can be computed from equation (3.7) and points (4) and (5) in section 3.3.1 above, viz. :

$$S_{xb} = \left(\frac{K_b}{K_b + K_s}\right) S_{xt} \qquad \ldots (3.11)$$

where $K_b = \ln\left(\frac{er}{\Delta_a}\right)$ for $b_1 = 1$

and $K_b = \left(\frac{1}{1-b_1}\right)\left(1 - b_1 \left(\frac{\Delta_a}{r}\right)^{(-b_1)}\right)$ for $b \neq 1$ $\qquad \ldots (3.12)$

$$K_s = 0.205 \ln\left(\frac{912d}{r}\right) \ln\left(\frac{d}{r}\right) \quad \text{for } b_1 = 1$$

and

$$K_s = 0.41 (1-b_1)^{-2} \left[(1-b_1)\left(\frac{d}{r}\right)^{1-b_1} \ln\left(\frac{30.2d}{r}\right) - 3.4\right) + \left\{1-\left(\frac{d}{r}\right)^{1-b_1}\right\}] \quad \text{for } b_1 \neq 1 \qquad \ldots (3.13)$$

b_1 was found empirically to be [15] :

$$b_1 = 1.05 \left(\frac{w}{\kappa v_{*wc}}\right)^{0.96} \left(\frac{r}{d}\right)^{0.013 \left(\frac{w}{\kappa v_{*wc}}\right)} \qquad \ldots (3.14)$$

3.4 Representative wave height

The *single representative wave*, which will yield the same resultant longshore sediment transport as the *complete wave spectrum* in the case of irregular wave attack, will again be a function of the boundary conditions. By assuming (1) a Raleigh-distributed wave height spectrum, and (2) the superposition of the transports generated by the individual waves in the spectrum, a *representative wave height* H_r was computed for the SWANBY-detail predictor in the same manner as in Chapter 2.
A design curve is presented in Figure 12, whereby it becomes possible to determine the *representative wave height* H_r in terms of the rms - wave conditions. The representative height varies between the median wave height (H_{50}) and the significant wave height (H_{sign}), with a tendency towards H_{sign} at the lower transport rates. Seeing that the lower waves in the spectrum will not transport sediment as readily in cases near the initiation of motion, this tendency is to be expected.
The single representative wave height for the SPM-overall predictor is by definition the rms wave height.

4. APPLICATION

4.1 *General*

Normally the losses from an area which had been replenished by a beachfill, can be estimated by using methods which are based on the *grain size distribution* of the *borrow* and *native material* only. The three most-used formulae in this category are those of *Krumbein-James* [10], which is suggested for use in the Shore Protection Manual [19], *Dean* [4] and *James* [8].

The Krumbein-James and Dean methods predict an *overfill ratio*, i.e. the ratio between the *volume of sediment* that has *to be placed* in order to retain the design volume and the *required design volume* of sediment in the fill. The Krumbein-James method assumes some portion of the borrow material (which has the same grain size distribution as the native material) to be absolutely stable and to stay on the beach indefinately, whereas the rest of the borrow material will be lost. The Dean-method, on the other hand, assumes that the borrow material which is coarser than the native material will *not be lost*.
James assumes that no material is absolutely stable, and that *fine material is less stable than coarse* material. He then computes a *relative retreat rate*, which is basically the ratio between the *loss rate* of the borrow material in the fill and that of the native material in the original beach profile.

In order to allow the comparison of the losses, as predicted by the techniques described in this paper, and those given by the above-mentioned three beachfill methods [10], [4], [8], the following two definitions were made :

$$\textit{Overfill Ratio (SEGAR)} = \frac{(\Delta S_y)_{borrow} + (\Delta S_x)_{borrow}}{V_{fill}} \quad \ldots (4.1)$$

and

$$\textit{Relative Retreat Rate (SEGAR)} = \frac{(\Delta S_y)_{borrow} + (\Delta S_x)_{borrow}}{(\Delta S_y)_{native} + (\Delta S_x)_{native}} \quad \ldots (4.2)$$

where (ΔS_y) and (ΔS_x) are the losses in the offshore and longshore directions respectively, and V_{fill} is the volume of sediment placed in the beachfill. When computing (ΔS_y) it should be kept in mind that the dimensions of the transport rates S_y in chapter 2 are $m^3/m/s$, while those in chapter 3 (S_x) are m^3/s. In equations (4.1) and (4.2) sediment is considered lost when it moves out of the area in which it was placed, *i.e.* that volume of sediment which has to be replaced in, for instance, an *annually recurring replenishment*. Due to the fact that the sediment moved in the offshore direction will eventually build a new equilibrium condition, which will conform to the borrow material and the wave climate, the annual losses, i.e. the required recurring replenishment, as characterized by equations (4.1) and (4.2), will gradually diminish with time. The present calculations only show the losses during the first replenishment period. The longshore losses were computed by both the SWANBY-detail predictor method and the SPM-overall predictor, whereafter a representative loss was computed from these two figures.

Due to the fact that both the *overfill ratio (SEGAR)* and the *relative retreat rate (SEGAR)* are time-dependent, a time-duration of 10 days was chosen as basis for the comparison, during which time one wave condition took place. When doing an actual beachfill design, the wave conditions in an average year should be applied *consecutively* to the gradually developing profile.

4.2 *Beachfill characteristics*

A typical beach profile for Natal (situated on the South African east coast) was taken as the initial profile for the computations. The geometry of the initial profile and the two beachfills, as well as the grain size characteristics, are given in Figure 13. As can be seen, six different cases result, viz. $\alpha_{borrow} = 1/10$ and $1/5$, each with $D_{50} = 200 \times 10^{-6}$, 500×10^{-6} and 1000×10^{-6}m. It was assumed that the beachfill has a longshore length $l_x = 1000$ m, and is situated in an area with no updrift supply of sediment. No gradients initiated by the placing of the fill itself, will be considered, i.e. edge effects at the longshore extremities of the fill will be neglected.

The wave condition in the area was taken to be :

$$(H_o)_{sign} = 2 \text{ m} \; ; \; T = 10 \text{ s} \; ; \; \theta_b = 5^o \; .$$

4.3 *Discussion of results*

The computed losses, as given by the various methods, are represented graphically in Figure 14. The following general observations regarding the results are relevant :

(1) The beachfill methods of Krumbein-James, Dean and James are all independent of the profile geometry, whereas the Krumbein-James and Dean methods are also independent of the wave climate. In the James-method the wave climate can perhaps be included via the choice of the measure of selectivity of the sorting process Δ (as defined by James [8]). Both the wave climate and the profile geometry do, however, influence the losses. Consequently, the above-mentioned three methods can only be used to obtain comparative results for various possible borrow materials.

(2) If all the consecutive wave conditions in an average year are taken into account, the resultant

losses will be lower than those given by the higher waves only, due to the fact that the lower waves will initiate an *onshore* sediment movement.

(3) Both the relative retreat rate (as given by *James*) and the overfill ratio (as given by Krumbein-James and Dean) are equal to unity in the case of a borrow material which is *identical* to the native material. The method presented in this paper (called the SEGAR-method) yields higher values of both the relative retreat rate and the overfill ratio (of approximately 2) in the case where the native and borrow materials are identical. This higher loss rate seems logical, seeing that the initial profile with fill is steeper than the initial profile alone (see Figure 13). Offshore losses will thus increase (re chapter 2).

(4) The relative retreat rates predicted by the James-method are appreciably smaller than those predicted by the SEGAR-method, for all values of D_{50} except $D_{50} = 200 \times 10^{-6}$m. A study of the original paper by James reveals that if $\Delta = 1.0$ as suggested in [8], the relative retreat rate is actually < 1 for $330 \times 10^{-6}\text{m} < (D_{50})_{borrow} < 1000 \times 10^{-6}$m, which is unfeasible from a physical viewpoint. For $(D_{50})_{borrow} < 200 \times 10^{-6}$m, on the other hand, the relative retreat rate R_b increases drastically to completely unrealistic values (for instance, for $D_{50} = 100 \times 10^{-6}$m; $M_{\phi_b} = 3.23$, $\sigma_{\phi_b} = 1.08$:- $R_b = 6.8 \times 10^3$ if $\Delta = .6$ and $R_b = 9.2 \times 10^4$ if $\Delta = 1.0$). As was already pointed out by James [8], the relative retreat rate is very dependent on the value of Δ. As Δ is mostly unknown, this represents a serious restriction in the applicability of the theory.

(5) The overfill ratios predicted by Dean and especially by Krumbein-James for values of $D_{50} < 500 \times 10^{-6}$m (in the present illustration), are exceedingly high. The Dean-method seems to have the soundest physical background of the two methods.

(6) The SEGAR-method described in the present paper can, if necessary, be used to obtain the relative losses in the offshore and longshore directions respectively, as the transports in both these directions are already computed. This is not possible for the Krumbein-James [10], Dean [4] and James [8] methods.

4.4 *Concluding remarks*

Although the SEGAR-method, which takes into account the local wave climate and the geometry of the beachfill, is more complicated to apply than the other three beachfill methods [10], [4] and [8], it yields results which seem to be more comparable with the known prototype behaviour of a beachfill area, than the results given by [10], [4] and [8]. It is accordingly suggested that the SEGAR-method is used for beachfill design. *Back-up computations, yielding comparative results only*, of both the *relative retreat rate* and the *overfill ratio*, can be made by using the *James-method* (provided that an appropriate choice of Δ can be made) and the *Dean-method* respectively. The Krumbein-James method generally over-predicts the overfill ratio, and is not recommended for use.

5. SUMMARY

Predictor techniques have been presented, whereby it is possible to compute *onshore-offshore* and *longshore sediment transports* respectively. These respective techniques can be used in combination to compute sediment losses in numerous applications. One such application, viz. to a beachfill problem, was described in detail. The results were shown to be realistic.

A *comparison of computed results with actual field measurements* at a beachfill location will be the logical next step in the testing of the techniques.

LIST OF REFERENCES

1. ACKERS, P. and WHITE, W.R. Sediment transport : New approach and analysis; Proc. ASCE Journal of the Hydraulics Division, HY 11, November 1973.

2. BIJKER, E.W. Some considerations about scales for coastal models with movable bed; Delft Hydraulics Laboratory, Publication No. 50 142 pp, November 1967.

3. DAS, M.M. Suspended sediment and longshore sediment transport data review; Proc. 13th Coastal Engineering Conference, Vancouver, Volume II, 1972.

4. DEAN, R.G. Compatibility of borrow material for beach fills, Proc. 14th Coastal Engineering Conference, Copenhagen, Volume II, 1974.

5. DE HAAN, Evaluatie zandtransporten bij eenparige stroming ("Evaluation of sediment transport for uniform flow"); Delft University of Technology, graduation thesis, to be published in 1976.

6. EAGLESON, P.S., GLENNE, B. and DRACUP, J.A. Equilibrium characteristics of sand beaches; Proceedings, ASCE, Journal of the Hydraulics Div., 89, Paper No. 3387, pp 35-57, January 1963.

7. GOLE, C.V., TARAPORE, Z.S. and DIXIT, J.G. Applicability of sediment transport formulae to natural streams; Proc. 15th Congress IAHR Istanbul, September 1973.

8. JAMES, W.R. Beach fill stability and borrow material texture; Proc. 14th Coastal Engineering Conference, Copenhagen, Volume II, 1974.

9. JONSSON, I.G. Wave boundary layers and friction factors; Proc. 10th Conference on Coastal Engineering, Tokyo, Volume I, Chapter 10, pp 127-148, 1966.

10. KRUMBEIN, W.C. and JAMES, W.R. A lognormal size distribution model for estimating stability of beach fill material; T.M.-16, U S Army, Corps of Engineers, Coastal Engineering Research Center, Washington, D.C., November 1965.

11. MOGRIDGE, G.R. and KAMPHUIS, J.W. Experiments on bed form generation by wave action; Proc. 13th Coastal Engineering Conference, Vancouver, Vol. 2, pp 1123-1142, 1972.

12. SILVESTER, R. Coastal Engineering, 2; Developments in Geotechnical Engineering, Vol. 4B; Elsevier Scientific Publishing Company, Amsterdam, 1974.

13. SWART, D.H. A schematization of onshore-offshore transport; Proc. 14th Coastal Engineering Conference, Copenhagen, June 1974.

14. SWART, D.H. Offshore transport and equilibrium beach profiles; Delft Hydraulics Laboratory, Publication No. 131, December 1974.

15. SWART, D.H. and DELFT HYDRAULICS LABORATORY. Coastal sediment transport : computation of longshore transport; Delft Hydraulics Laboratory Report R968, November 1975.

16. SWART, D.H. Weighted value of depth of initiation of movement; Unpublished note, June 1976.

17. SWART, D.H. Sediment transportation in the coastal environment; Lecture notes for postgraduate ECOR-course in Coastal Engineering, Port Elizabeth, South Africa, June 1976.

18. TASK COMMITTEE FOR PREPARATION OF SEDIMENT MANUAL. Sediment transportation mechanics : H. Sediment discharge formulae; Proc. ASCE, Journal of the Hydraulics Division, Vol 97, HY 4, April 1971.

19. U.S. ARMY COASTAL ENGINEERING RESEARCH CENTER. Shore Protection Manual, Vol. 1 - 3; U.S. Government Printing Office, 1973.

20. WHITE, W.R., MILLI, H. and CRABBE, A.D. Sediment transport : an appraisal of available methods, Volumes 1 and 2; Hydraulics Research Station, Wallingford, Report INT 119, November 1973.

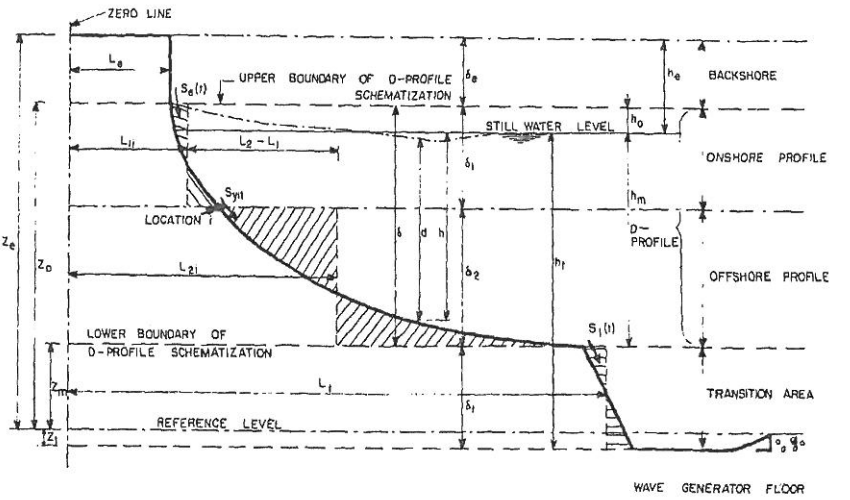

Figure 1 : Schematization of beach profile at time t

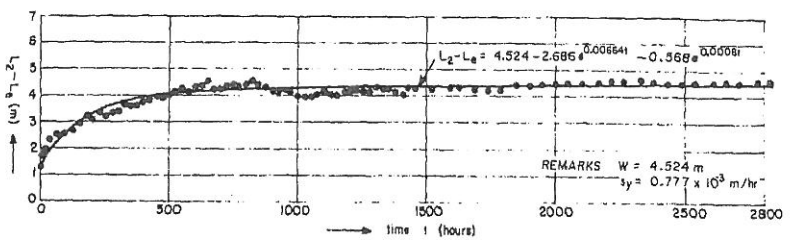

$\delta_1 = \delta_0 = 0.22\,m$; $\delta_2 = \delta = 0.25m$

Figure 2 : Schematized time-variation of sediment in D-profile

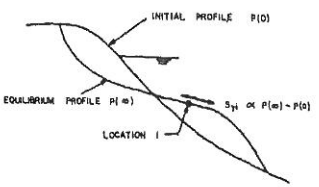

Figure 3 : Relationship between transport S_{yi} and profile form

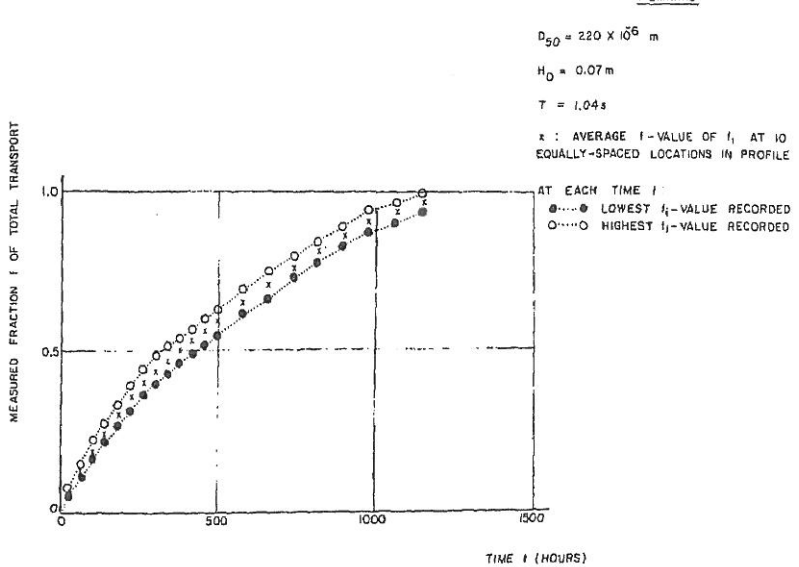

Figure 4 : Time- and depth-variation of measured fractions f_i

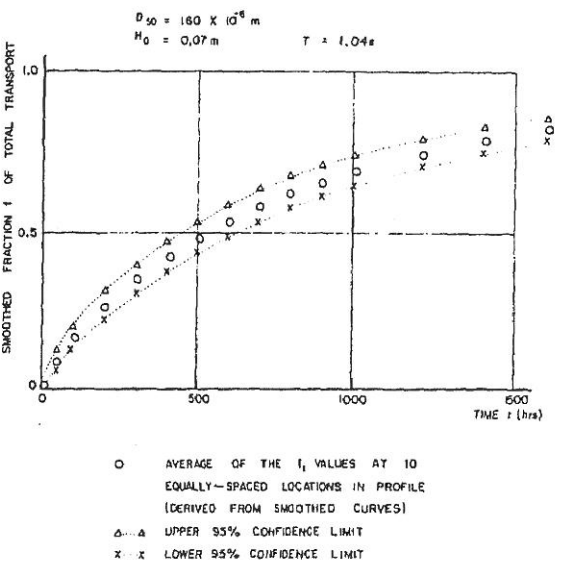

Figure 5 : Time- and depth-variation of smoothed fraction f_i

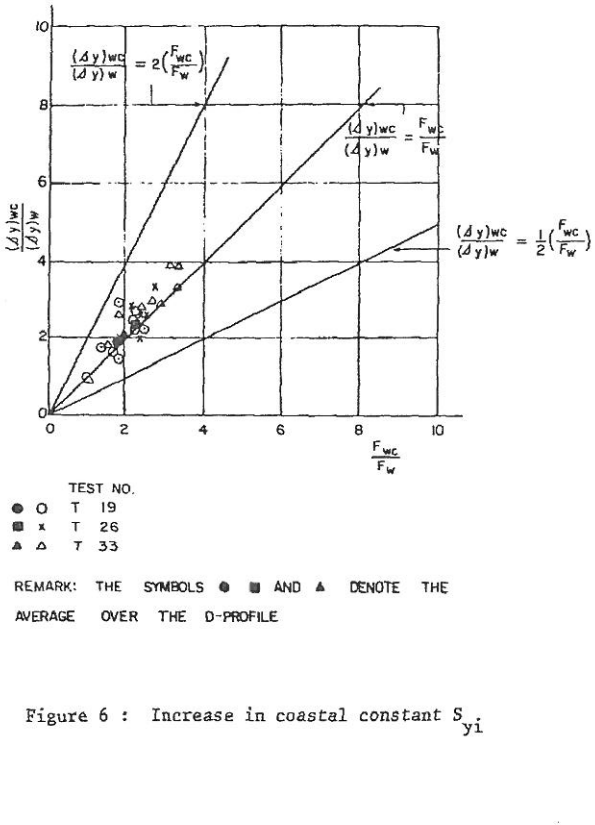

Figure 6 : Increase in coastal constant S_{yi}

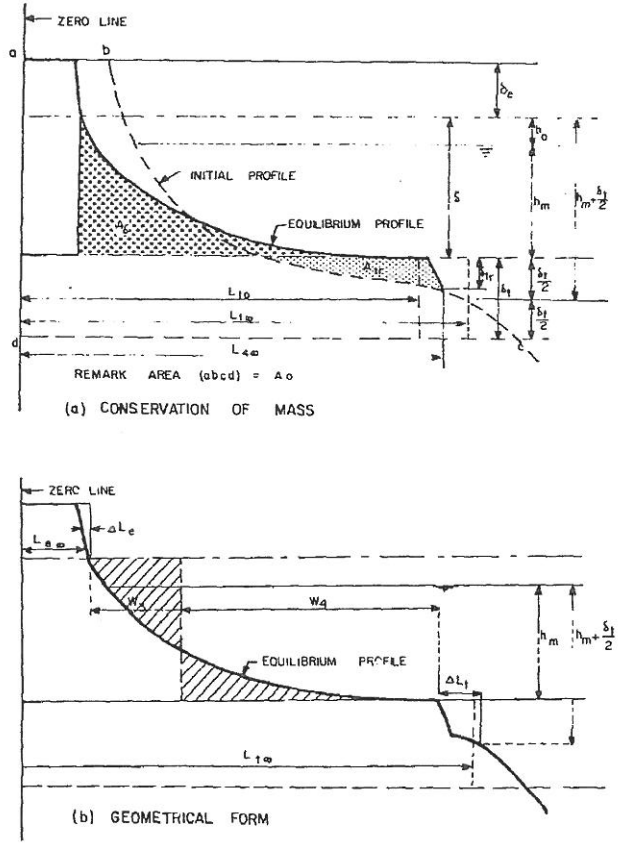

Figure 7 : Definition sketch: computation of W_e, W_t and δ_{tr}

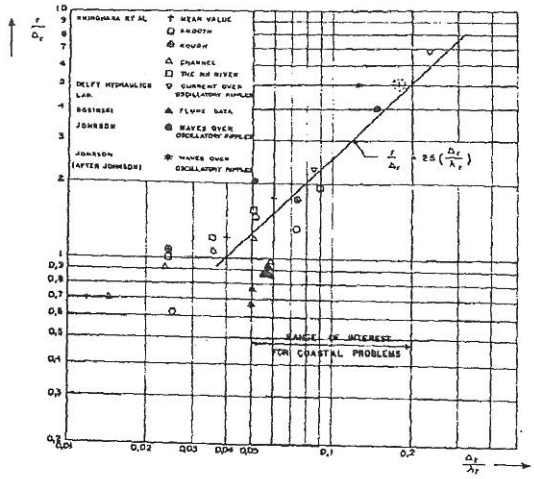

Figure 8 : Computation of relative roughness

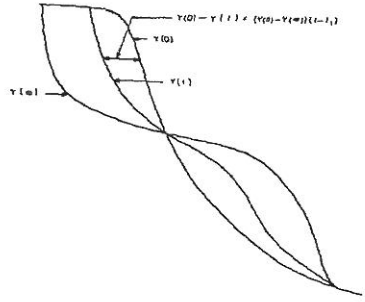

Figure 9 : Computation of time-dependent profiles

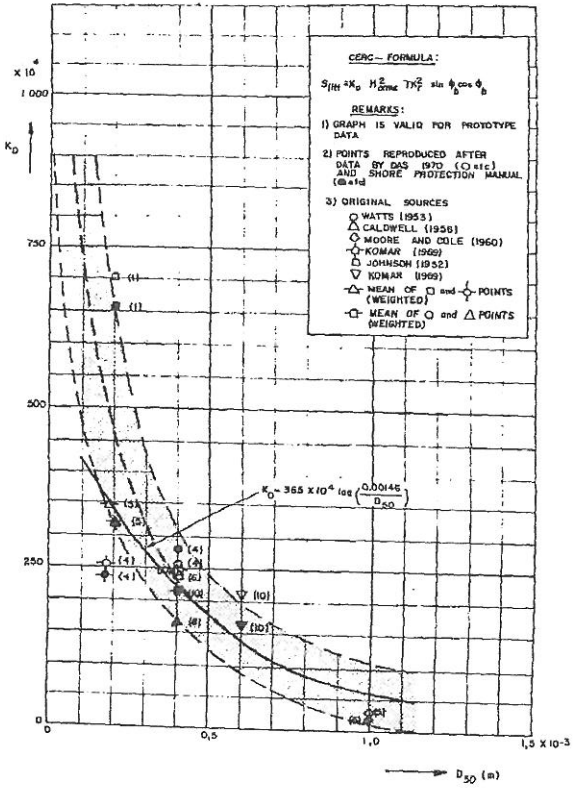

Figure 10 : Grain-size dependence of K_o

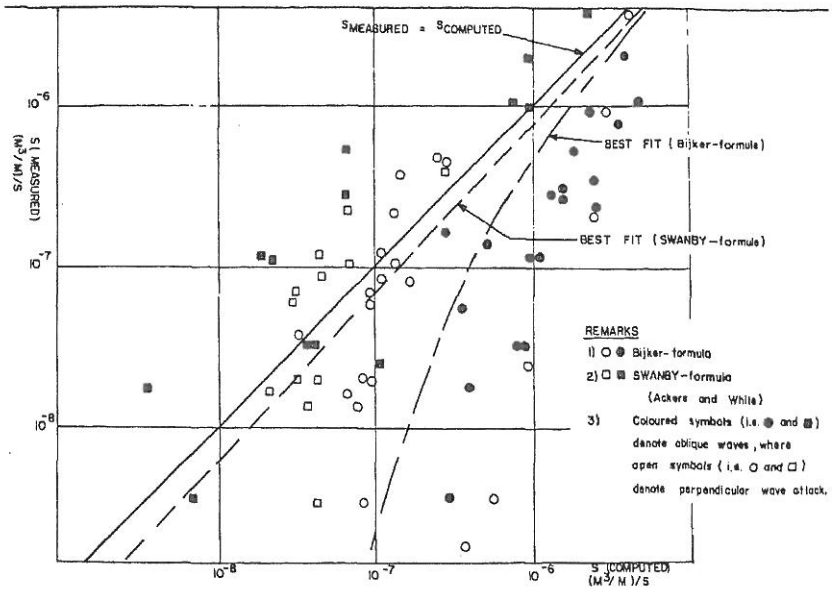

Figure 11 : Comparison between measured and computed longshore transport rates

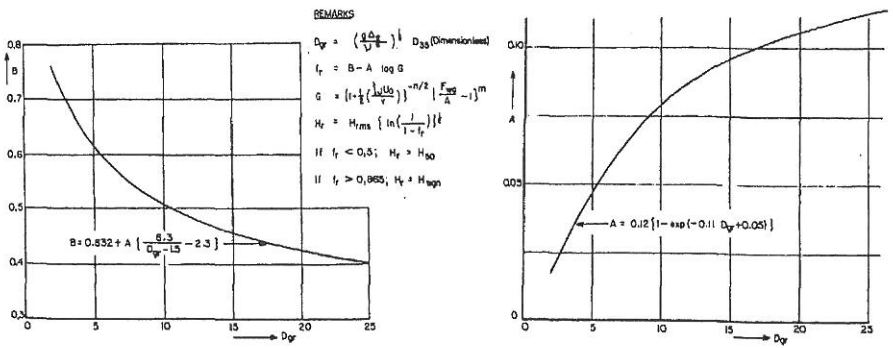

Figure 12 : Computation of representative wave height H_r

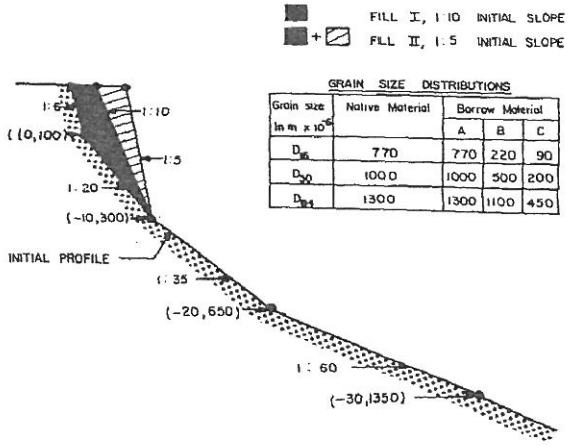

GRAIN SIZE DISTRIBUTIONS

Grain size in m x 10^{-6}	Native Material	Borrow Material		
		A	B	C
D_{16}	770	770	220	90
D_{50}	1000	1000	500	200
D_{84}	1300	1300	1100	450

Figure 13 : Characteristics of beachfill

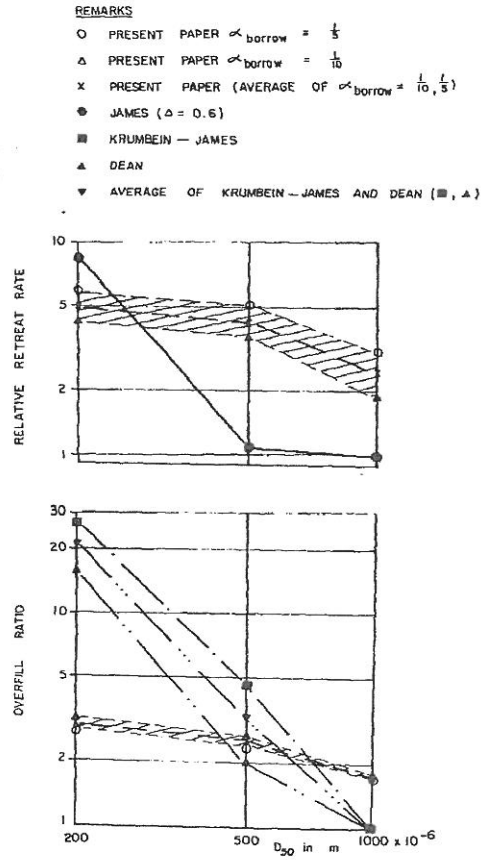

Figure 14 : Beachfill-stability results